Evaluation of the nephrotoxicity and safety of low-dose aristolochic acid, extending to the use of Xixin (Asurum), by determination of methylglyoxal and D-lactate

Chia-En Lin
Taipei Medical University
Po-Yeh Lin
Taipei Medical University
Wen-Chi Yang
Taipei Medical University
Yu-Shen Huang
Taipei Medical University
Tzu-Yao Lin
Taipei Medical University
Chien‐Ming Chen
National Taipei University of Technology
Hung-Shing Chen
National Taiwan University of Science and Technology
Jen-Ai Lee
Taipei Medical University
Shih-Ming Chen (smchen@tmu.edu.tw)
Taipei Medical University College of Pharmacy https://orcid.org/0000-0002-0273-4847

Research

Keywords: Aristolochic acid (AA), D-lactate, fibrosis, methylglyoxal, nephrotoxicity

Posted Date: July 29th, 2020

DOI: https://doi.org/10.21203/rs.3.rs-48442/v1

Version of Record: A version of this preprint was published at Journal of Ethnopharmacology on May 1st, 2021. See the published version at https://doi.org/10.1016/j.jep.2021.113945.

Evaluation of the nephrotoxicity and safety of low-dose aristolochic acid, extending to the use of Xixin (*Asurum*), by determination of methylglyoxal and D-lactate

Chia-En Lin[a], Po-Yeh Lin[a], Wen-Chi Yang[a], Yu-Shen Huang[a], Tzu-Yao Lin[a], Chien-Ming Chen[b], Hung-Shing Chen[c], Jen-Ai Lee[a,*], Shih-Ming Chen[a,*]

[a] School of Pharmacy, College of Pharmacy, Taipei Medical University, No.250 Wu-Hsing Street, Taipei 110, Taiwan

[b] Department of Electro-Optical Engineering, National Taipei University of Technology, Taipei, Taiwan

[c] Graduate Institute of Electro-optical Engineering, National Taiwan University of Science and Technology, No.43, Keelung Rd., Sec.4, Da'an Dist., Taipei, Taiwan

[*]Corresponding author. Tel./fax: +886-2-2736-1661 ext.6176.

E-mail address: smchen@tmu.edu.tw (Shih-Ming Chen).

[*]Additional corresponding author. Tel./fax: +886-2-2736-1661 ext.6125.

E-mail address: jenai@tmu.edu.tw (Jen-Ai Lee).

Co-author E-mail: Chia-En Lin (d301106002@tmu.edu.tw) ; Po-Yeh Lin (poyeh0111@gmail.com); Wen-Chi Yang (gigyang311@gmail.com); Yu-Shen

Huang (danny7781@gmail.com) ;Tzu-Yao Lin (b323102012@tmu.edu.tw); Chien-Ming Chen (cmchen@mail.ntut.edu.tw); Hung-Shing Chen (bridge@mail.ntust.edu.tw).

Abstract

Background: Most *Aristolochiaceae* plants are prohibited due to aristolochic acid nephropathy (AAN), except Xixin (*Asarum spp.*). Xixin contains trace amounts of aristolochic acid (AA) and is widely used in Traditional Chinese Medicine. Methylglyoxal and D-lactate are regarded as biomarkers for nephrotoxicity. Thus, this study aimed to evaluate tubulointerstitial injury and interstitial renal fibrosis by determining urinary methylglyoxal and D-lactate after withdrawal of low-dose AA in a chronic mouse model.

Methods: C3H/He mice in the AA group (n = 24/group) were given *ad libitum* access to distilled water containing 3 μg/mL AA (0.5 mg/kg/day) for 56 days and drinking water from days 57 to 84. The severity of tubulointerstitial injury and fibrosis were evaluated using the tubulointerstitial histological score (TIHS) and Masson's trichrome staining. Urinary and serum methylglyoxal were determined by high-performance liquid chromatography (HPLC); urinary D-lactate were determined by column-switching HPLC.

Results: After AA withdrawal, serum methylglyoxal in the AA group increased from day 56 (429.4 ± 48.3 μg/L) to 84 (600.2 ± 99.9 μg/L), and peaked on day 70 (878.3 ± 171.8 μg/L; $p < 0.05$); TIHS and fibrosis exhibited similar patterns. Urinary methylglyoxal was high on day 56 (3.522 ± 1.061 μg), declined by day 70 (1.583 ± 0.437 μg) and increased by day 84 (2.390 ± 0.130 μg). Moreover, urinary D-lactate was elevated on day 56 (82.10±18.80 μg) and higher from day 70 (201.10 ± 90.82 μg) to 84 (193.28 ± 61.32 μg).

Conclusions: Methylglyoxal is induced after AA-induced tubulointerstitial injury, thus methylglyoxal excretion and metabolism may be a detoxification and repair strategy. A low cumulative AA dose is the key factor that limits tubulointerstitial injury and repair. Thus, AA-containing herbs, especially Xixin, should be used at low doses for short durations (less than one month).

Keywords: Aristolochic acid (AA), D-lactate, fibrosis, methylglyoxal, nephrotoxicity

Background

Aristolochiaceae plants are traditionally used in several Traditional Chinese Medicine (TCM) formulas, such as Xiao-Qing-Long-Tang, Chuan Xiong Cha Tiao San, Ma Huang Fu Zi Xi Xin Tang, Qing Shang Juan Tong Tang and Du Hwa Jih Sheng Tang. However, as they induce aristolochic acid nephropathy (AAN), most

aristolochic acid (AA)-containing plants is prohibited, including *Aristolochia contorta* (Ma Dou Ling) [1], *Aristolochia fangchi* (Guang Fang Ji) [1], *Aristolochia manshuriensis* (Guan Mu Tong) [1], *Aristolochia contorta* (Tian Xian Teng) and *Aristolochia debilis* (Qing Mu Xiang) [1]. These species can be replaced in Traditional Chinese Medicine (TCM) by other non-*Aristolochiaceae* plants [2]. However, Xixin cannot be replaced by other non-*Aristolochiaceae* plants. All origins of Xixin, including *Asarum heterotropoides* Fr. Schmidt var. mandshuricum (Maxim.) Kitag, *Asarum crispulatum* C.Y. Cheng and C.S. Yang, *Asarum forbesii* Maxim, *A. himalaicum* Hooh. F. and Thoms. Ex Klotzsch, *Asarum sieboldii* Miq, *Asarum debile* Franch *Asarum maximum* Hemsl, *Asarum ichangense* C.Y. Cheng and C.S. Yang, and *Asarum fukienense* C.Y. Cheng and C.S. Yang, are members of the *Aristolochiaceae* family. Moreover, Xixin and its combination with other herbs are frequently used to treat a variety of conditions, including fever [3], influenza in the elderly [4], infection [5], allergy [6], caries [7], inflammation [8, 9], pain [8], rhinitis [9] and rheumatoid arthritis [10]. Consequently, while the use of AA-related products, especially Xixin, remains essential, their safety is controversial.

Methylglyoxal and D-lactate can be used to assess nephrotoxicity and play key roles in the progression of renal injury, including diabetic [11], gentamicin-induced [12], Pb-induced [13] and acute AA-induced nephropathy [14-16]. The highly reactive

77 dicarbonyl groups of methylglyoxal denature proteins and nucleic acids; the resulting
78 methylglyoxal-derived compounds are called advanced glycation end products
79 (AGEs) [17]. As a mechanism to limit the toxicity of methylglyoxal, methylglyoxal is
80 metabolized into D-lactate via the glyoxalase system [18, 19]. Thus, D-lactate is
81 considered to be a marker of renal damage and accumulation of methylglyoxal. On
82 the other hand, renal injury increases both D-lactate and L-lactate, while prednisolone
83 [18] or metformin [10] treatment alleviate histological damage and decrease D-lactate
84 —rather than L-lactate or D/L-lactate—in AAN models. Nevertheless, the changes in
85 methylglyoxal and D-lactate contents after long-term administration of AA have not
86 been explored, although elevation of urinary D-lactate was observed in a previous
87 study [20].
88 This study aimed to explore whether the progression of tubulointerstitial injury
89 and interstitial renal fibrosis stop and/or reverse after discontinuing 56-day
90 administration of low-dose AA by determining the contents of urinary methylglyoxal
91 and D-lactate. The results of this study may help to identify the safe dose and duration
92 of administration of AA-related products, especially Xixin.
93
94 **Methods**
95 **Materials and chemicals**

Animal experiments

All animal protocols were approved by the Animal Care and Use Committee of Taipei Medical University (LAC-2019-0482). Six-week-old female C3H/He mice were obtained from the National Laboratory Animal Breeding and Research Center (Taipei, Taiwan) and randomly allocated to either the normal group (N) or the AA group (n = 24/group) [20]. Six mice in the same group were placed in per cage. These mice were placed in temperature-controlled (25 ± 2°C) and humidity-controlled (65 ± 5%) rooms with a 12:12 light-dark photoperiod, and had access to standardized food pellets (Fwusow Industry Co., LTD., Taichung, Taiwan). The AA group were given *ad libitum* access to distilled water containing 3 μg/mL AA (Sigma-Aldrich, Inc., MO, USA; AAI:AAII = 63:31; 0.5 mg/kg/day) as drinking water for 56 days. After day 56, the AA group mice received normal drinking water [20, 21]. The N group received only normal drinking water. Urine samples were collected over 12 hours on days 28, 56, 70, and 84 using a metabolic cage (Tokiwa Chemical Industries Co. Ltd., Japan). The mice were humanely sacrificed on day 28, 56, 70 or 84 (n = 6/group). Whole blood samples were collected and the kidneys were excised [20, 21].

Biochemical parameters

The Blood Urea Nitrogen Kit (Beckman Coulter, Brea, California, USA) was used to determine blood urea nitrogen (BUN). Urinary *N*-acetyl-β-D-glucosaminidase (NAG) activity, i.e., production of 4-methylumbelliferone (4-MU) from 4-methylumbelliferyl-*N*-acetyl-β-D-glucosaminide within 15 min, was reacted in 100 mM citrate buffer (pH 4.6-5.0). The reaction was stopped by addition of 200 mM glycine buffer (pH 10.4-10.6) and fluorescence was measured at 460 nm after excitation at 370 nm [21].

Serum creatinine (Scr) was determined using a modified version of the previous protocol [14, 22]. Briefly, 20 μL blood samples were mixed with 10 μL of 1 mM cimetidine·HCl (Sigma-Aldrich, Inc., MO, USA) as an internal standard [I.S.] and 170 μL acetonitrile (MeCN) and centrifuged at 700 *g* for 15 min at 4°C. The supernatants (50 μL) were injected into the UV-HPLC system, which included an L-7100 Pump (Hitachi, Tokyo, Japan), L-2200 Intelligent Autosampler (Hitachi), TSKgel ODS-80Ts column (250 × 4.6 mm i.d., 5 μm; Tosoh Co., Tokyo, Japan) and an 875-UV Intelligent UV/VIS Detector (JASCO International Co., Ltd., Tokyo, Japan). The mobile phase was 36:60 (v/v) MeCN/30 mM sodium lauryl sulfate $_{(aq)}$:100 mM sodium dihydrogen phosphate $_{(aq)}$ (pH 3.0) and the flow rate was 0.8 mL/min. The fractions were monitored at 234 nm.

Histological examinations

133 Half of each left kidney was fixed in 10% buffered neutral formalin solution for
134 24 h at 4°C, embedded in paraffin, sectioned at 4-5 μm and stained with periodic
135 acid–Schiff (PAS) (Muto Pure Chemicals Co., Ltd., Tokyo, Japan), Masson's
136 trichrome (Muto Pure Chemicals Co., Ltd., Tokyo, Japan), or Picro Sirius Red
137 Staining Kit (CIS-Biotechnology Co., Ltd., Taichung, Taiwan) according to the
138 instruction of manufactures [20, 21]. Sections were observed at a magnification of
139 200× using a G-330 light microscope (Optima, New Taipei City, Taiwan) and images
140 were captured using a Nikon Coolpix 4500 camera (Nikon, Tokyo, Japan) [20, 21].

141 **Tubulointerstitial histological score**

142 The tubulointerstitial histological score (TIHS) was used to evaluate the severity
143 of tubulointerstitial damage in the PAS-stained sections. Ten non-overlapping fields of
144 view were scored for each mouse. The TIHS assesses three major items: the severity
145 of mononuclear cell infiltration into the interstitium (0, absent; 1, few scattered cells;
146 2, groups of mononuclear cells; and 3, dense widespread infiltrate); the severity of
147 degeneration in the tubular epithelium (0, no degeneration of the tubular epithelium;
148 1, one group or a single degenerated tubule; 2, several clusters of degenerated tubules;
149 3, moderate degeneration of the tubular epithelium; 4, more severe degeneration of
150 the tubular epithelium; and 5, extremely severe degeneration of the tubular
151 epithelium, with massive necrosis and atrophy); and the severity of interstitial fibrosis

(0, absent; 1, mild diffuse fibrosis; 2, moderate fibrosis; and 3, severe fibrosis). The THIS of each mouse was expressed as the sum of the three scores [14, 15, 20, 21, 23].

Semi-quantitative analysis of fibrosis

Interstitial renal fibrosis was assessed in the Masson trichrome and Picro Sirius Red-stained sections by determining the percentage area positive for aniline blue and red in ten non-overlapping fields of view for each mouse using ImageJ (National Institutes of Health, MD, USA), respectively [20].

Determination of methylglyoxal

Urinary and serum methylglyoxal were determined by high-performance liquid chromatography with fluorescence detection (FD-HPLC). The FD-HPLC system (Hitachi, Tokyo, Japan) was composed of L-2130 Pump, L-2200 Intelligent Autosampler and L-2480 Fluorescence Detector [13, 20].

Briefly, the serum and urine samples were fluorogenically derivatized with 6-diamino-2,4-dihydroxypyrimidine sulfate (DDP) for 30 min at 60 °C, the reactions were stopped with 0.01 M citric acid (pH 6.0) and 20 μL samples were loaded onto the ODS column (250 × 4.6 mm, 5 μm particle size; Biosil Chemical Co. Ltd., Taipei, Taiwan) at 33 °C [24]. The mobile phase was 97:3 (v/v) 0.01 M citric acid buffer (pH 6.0) and MeCN and the flow rate was 0.7 mL/min. The fractions were monitored at an emission wavelength of 500 nm and excitation wavelength of 330 nm. Urinary

171 methylglyoxal content was expressed as the level of methylglyoxal × 12 h-urinary
172 volume [20].

173 **Determination of D-lactate**

174 **Florigenic derivatization of lactate**

175 Urine samples (20 μL) were mixed with 10 μL of 1 mM propionic acid as an
176 internal standard (I.S.) and 170 μL of acetonitrile (MeCN) and centrifuged at 700 g
177 for 10 min at 4 °C. For florigenic derivatization, 100 μL of the supernatant was
178 incubated with 100 μL of 8 mM 4-nitro-7-piperazino-2,1,3-benzoxadiazole (NBD-PZ)
179 in MeCN in 25 μL of 280 mM triphenylphosphine (TPP) and 25μL of 280 mM 2,2'-
180 dipyridyl disulfide (DPDS) in MeCN. After 3 h, 250 μL of 0.1% aqueous
181 trifluoroacetic acid (TFA) was added to stop the reaction. To remove excess NBD-PZ,
182 100 μL of the solution was passed through a MonoSpin™ SCX cartridge (GL Science
183 Inc., Tokyo, Japan) and the eluates were collected [20, 25].

184 **Isolation of D,L-lactate and D-lactate**

185 Urinary D-lactate were determined using a column-switching FD-HPLC system
186 by first isolating D,L-lactate and then separating D-lactate. NBD-PZ-fluorogenic
187 derivatized samples (20 μL) were loaded into an L-7100 Pump (Hitachi, Tokyo,
188 Japan), L-2200 Intelligent Autosampler (Hitachi, Tokyo, Japan), Biosil ODS column
189 (4.6 × 250 mm, 5 μm; Biotic Chemical Co., Ltd., Taipei, Taiwan) and L-2485

190 Fluorescence Detector (Hitachi, Tokyo, Japan) to determine D,L-lactate (total lactate)
191 [20, 25]. Mobile phase A was 12:20:68 (v/v/v) MeCN/MeOH/H_2O and mobile phase
192 B was 100% MeCN. The program was mobile phase A at 0.7 mL/min from 0 to 35
193 min, mobile phase A at 0.9 mL/min from 35.1 to 60 min, mobile phase B at 0.8
194 mL/min from 60.1 to 75 min, and mobile phase A at 0.7 mL/min from to 75.1 to 90
195 min. The D,L-lactate fraction was switched into the second part of the column-
196 switching FD-HPLC system using a six-valve switcher.
197 The second part of the FD-HPLC was L-7100 Pump (Hitachi, Tokyo, Japan),
198 Chiralpak ADRH column (150 × 4.6 mm, 5 μm particle size; Daicel Co., Osaka,
199 Japan) and L-2485 Fluorescence Detector (Hitachi, Tokyo, Japan). D-lactate and L-
200 lactate were separated using 60:40 (v/v) MeCN/H_2O as the mobile phase at a flow rate
201 of 0.3 mL/min. The NBD-PZ derivatives were detected using an emission wavelength
202 of 547 nm and excitation wavelength of 491 nm in both parts of the two-dimensional
203 FD-HPLC system. The D,L-lactate and D-lactate levels were based on the areas of the
204 corresponding peaks (D-7500 Integrator; Hitachi, Tokyo, Japan). Thus, the actual
205 amount of D,L-lactate was D,L-lactate level × 12-h urinary volume; the actual amount
206 of D-lactate was D-lactate level × 12-h urinary volume [20].
207 **Western blotting of glyoxalase 1**

208 Briefly, kidney homogenates were prepared and protein concentrations were
209 measured using the Pierce™ BCA Protein Assay Kit (Thermo Fisher Scientific,
210 Waltham, MA, USA). The samples (10 μg protein per lane) were separated on 12%
211 sodium dodecyl sulfate-polyacrylamide gels and electrophoretically transferred onto
212 Immun-Blot PVDF Membranes (Bio-Rad Laboratories, Inc., Hercules, CA, USA)
213 [21]. The antibodies used were anti-glyoxalase 1 antibody (GLO1; GTX105792;
214 GeneTex, Irvine, CA, USA; 1:1000), anti-β-actin antibody (20536-1-AP; Proteintech,
215 Rosemont, IL, USA; 1:2000) and goat anti-rabbit IgG (H+L) HRP conjugate antibody
216 (SA00001-2; Proteintech, Rosemont, IL, USA ; 1:4000). TOOLSensitive ECL Kit
217 (Tools Biotechnology co. Ltd., New Taipei City, Taiwan) was used detect the bands.
218 The intensity of the bands were measured using Image J (National Institute of Health,
219 Bethesda, Maryland, USA) and the levels of GLO1 were normalized to β-actin and
220 expressed relative to the N group.

221 **Statistical analysis**

222 All values were expressed as means ± standard deviation. The differences
223 between the N and AA groups were assessed using the Student's t-test at each time
224 point. Repeated measures ANOVA was used to compare the mean values of the
225 variables in the same group on Day 56, 70, and 84. P-values less than 0.05 were

defined as significant. SPSS for Windows 19th version (IBM Co., New York, NY, USA) was used to analyze all data.

Results

Biochemical parameters

All biochemical parameters (BUN, Scr, and NAG) were significantly elevated in the AA group compared to the N group on days 28, 56, 70 and 84 (Table 1). There were no significant differences in the BUN and Scr contents of the AA group on day 56 (24.13 ± 1.21 mg/dL and 0.283 ± 0.041 mg/dL), day 70 (25.83 ± 1.17 mg/dL and 0.317 ± 0.075 mg/dL), and day 84 (24.99 ± 0.98 mg/dL and 0.300 ± 0.063 mg/dL). In the AA group, urinary NAG activity was higher on day 56 (2.079 ± 0.089 U/L) and day 70 (2.297 ± 0.266 U/L) than on day 84 (1.895 ± 0.110 U/L).

Histological examination

PAS stained kidney sections (Fig. 1) indicated exposure to AA induced interstitial renal fibrosis, with the most severe fibrosis observed on day 70 (Fig. 1f). The PAS staining sections revealed severe renal damage in the AA group, including cellular infiltration, epithelial damage and interstitial renal fibrosis. There was a slightly cell infiltration and tubular atrophy on day 28, but no significant difference in TIHS between AA (0.8 ± 0.6) and N (0.2 ± 0.4) groups (Fig. 1a,1b,1f). The AA group

had significantly higher TIHS than the N group on day 56 (AA: 3.6 ± 0.7 *vs.* N: 0.2 ± 0.4; $p < 0.01$), day 70 (AA: 6.3 ± 0.8 *vs.* N: 0.3 ± 0.7; $p < 0.01$), and day 84 (AA: 4.6 ± 0.5 *vs.* N: 0.3 ± 0.7; $p < 0.01$) (Fig. 1f). The TIHS of the AA group increased between day 28 and day 70 and then reduced by day 84 (Fig. 1f).

Masson's trichrome staining was performed to semi-quantitatively analyze collagen deposition (Fig. 2). There was no significant difference in collagen deposition between AA (3.6 ± 0.2%) and N (3.5 ± 0.4%) groups on day 28 (Fig. 2a,b,i). Collagen deposition was significantly higher in the AA group than the N group on day 56 (AA: 14.1 ± 2.3% *vs.* N: 3.6 ± 0.5%; $p < 0.01$), day 70 (AA: 28.5 ± 3.5% *vs.* N: 3.8 ± 0.4%; $p < 0.01$), and day 84 (AA: 20.6 ± 1.6% *vs.* N: 4.0 ± 1.0%; $p < 0.01$) (Fig. 2i). In the AA group, higher levels of collagen deposition were detected on day 70 (Fig. 2f) than on days 56 (Fig. 2d) and 84 (Fig. 2h). Moreover, collagen deposition was also assessed by Picro Sirius Red staining (Fig. 3), and the findings were similar to Masson's trichrome staining. There was no significant difference in collagen deposition between AA (5.86 ± 1.38%) and N (5.72 ± 1.20%) groups on day 28 (Fig. 3a,b,i). The collagen deposition was significantly higher in the AA group than the N from day 56 (AA: 11.3 ± 1.2% *vs.* N: 6.5 ± 1.3%; $p < 0.05$) to day 84 (AA: 15.7 ± 1.5% *vs.* N: 6.4 ± 1.5%; $p < 0.05$) (Fig. 3i). The highest levels of collagen deposition in the AA group on day 70 (Fig. 3f), and the collagen deposition

264 significantly decreased from day 70 (21.9 ± 1.6%) to day 84 (15.7 ± 1.5%) ($p < 0.05$)
265 (Fig. 3i).

266 **Methylglyoxal in serum and urine**

267 The AA group had a higher serum methylglyoxal level than the N group on day
268 56 (AA: 429.4 ± 48.3 μg/L *vs.* N: 311.9 ± 29.2 μg/L; $p < 0.05$), day 70 (AA: 878.3 ±
269 171.8 μg/L *vs.* N: 373.1 ± 52.9 μg/L; $p < 0.01$), and day 84 (AA: 600.2 ± 99.9 μg/L *vs.*
270 N: 386.6 ± 61.5 μg/L; $p < 0.05$) (Fig. 4d). In the AA group, the serum methylglyoxal
271 level content significantly increased between day 56 and day 70 and declined between
272 day 70 and day 84 (Fig. 4d).

273 The AA group had higher urine methylglyoxal contents than the N group on day
274 56 (AA: 3.522 ± 1.061 μg *vs.* N: 1.408 ± 0.135 μg; $p < 0.05$) and day 84 (AA: 2.390 ±
275 0.130 μg *vs.* N: 1.630 ± 0.081 μg; $p < 0.05$) (Fig. 4h). There was no significant
276 difference in the urinary methylglyoxal contents of the AA (1.583 ± 0.437 μg) and N
277 groups (1.386 ± 0.255 μg) on day 70 (Fig. 4h). The urinary methylglyoxal content of
278 the AA group significantly decreased between day 56 and 70 and significantly
279 increased between day 70 and 84 (Fig. 4h).

280 **Urinary D,L-lactate and D-lactate contents**

281 The AA group had significantly higher urinary D,L-lactate contents than the N
282 group on day 56 (AA: 994.1 ± 161.0 μg *vs.* N: 151.9 ± 71.1 μg; $p < 0.001$), day 70

283 (AA: 1598.9 ± 396.0 μg *vs.* N: 125.8 ± 57.4 μg; $p < 0.001$), and day 84 (AA: 1447.0 ±
284 531.4 μg *vs.* N: 141.5 ± 48.6 μg; $p < 0.001$) (Fig. 5g). There was no significant change
285 in the urinary D,L-lactate content of the N group from day 56 to 84. However, the
286 urinary D/L-lactate content of the AA group significantly increased between day 56
287 and day 70 ($p < 0.05$) and remained high at day 84 (Fig. 5g).
288 The urinary D-lactate contents of the AA group were significantly higher than
289 those of the N group on day 56 (AA: 82.10 ± 18.80 μg *vs.* N: 5.88 ± 3.40 μg; $p <$
290 0.001), day 70 (AA: 201.09 ± 90.82 μg *vs.* N: 5.78 ± 2.77 μg; $p < 0.001$), and day 84
291 (AA: 193.28 ± 61.32 μg *vs.* N: 7.15 ± 3.28 μg; $p < 0.001$) (Fig. 5h). The urinary D-
292 lactate amount of the N group did not significantly change between day 56 and 84.
293 However, the urinary D-lactate amount of the AA group significantly increased
294 between day 56 to 70 ($p < 0.05$) and remained high at day 84 (Fig. 5h).
295 **Expression of GLO1**
296 The relative levels of GLO1 in the kidney of the AA group on day 56 (180.9 ±
297 12.8%), day 70 (150.8 ± 14.9%), and day 84 (167.2 ± 13.3%) were significantly
298 higher than the N group (100.0 ± 9.0%; $p < 0.05$) (Fig. 6b).
299
300 **Discussion**

The cumulative dose of AA administered to the mice in this study was approximately 0.56 mg (equivalent to 136.22 mg in humans), which is similar to the human study by Vanhaelen *et al.* (about 130 mg) [26]. The concentration of AA in Xixin depends on the origin (*A. heterotropoides*, *A. crispulatum*, *A. forbesii*, *A. himalaicum*, *A. sieboldii*, *A. debile*, *A. maximum*, *A. ichangense*, *A. fukienense*) [27], the portion of the plant used (roots, rhizomes, petioles, leaves) [28], and the extraction solvent (water, methanol) [28], thus the concentration of AA in Xixin ranges from trace to 3376.9 ppm [27, 28]. In patients receiving Xixin containing the highest concentrations of AA, intake of 38.5 g Xixin crude herbs can lead to interstitial renal fibrosis or urothelial carcinoma. Moreover, most TCM doctors use concentrated granules rather than the crude herbs. Additionally, while the regulations states that only the roots of Xixin should be used due to their lower AA content, whole plants are still available in markets [28]. Thus, it is necessary to determine the AA concentrations of Xixin crude herbs and concentrated granule samples.

Several animal studies have revealed that higher doses or longer durations of AA administration lead to severe AAN. In a rabbit model, renal hypocellular interstitial fibrosis was induced by intraperitoneal injection of AA (0.1 mg/kg/day) five times a week for more than 17 months [29], a much longer duration than the current study (56 days). Interstitial fibrosis was also induced in rats by subcutaneous administration of

AA (10 mg/kg/day) for five weeks; however, the changes after withdrawal of AA were not observed [30, 31]. In the current study, slight elevation of biochemical parameters were observed but rare fibrosis by day 28, compared to those on day 56 and 70. Moreover, while another acute mouse model used a much higher dose (10 mg/kg/day) than the current study (0.5 mg/kg/day), tubular necrosis—but rarely interstitial renal fibrosis—were observed after intravenous administration of AA for five days [14, 16]. Consequently, administration of a low cumulative dose (i.e., a low dose for a short period) of Xixin and monitoring NAG and renal function are essential to avoid exacerbation of tubulointerstitial injury.

Methylglyoxal and D-lactate are regarded as biomarkers for nephropathy and diabetes, thus most previous studies focused on how methylglyoxal is induced endogenously, how methylglyoxal reacts with proteins and nucleic acids to produce AGEs [27], and testing drugs that may lower methylglyoxal contents. Therefore, urinary excretion of methylglyoxal and D-lactate are considered to reflect excessive production of methylglyoxal due to renal injury and inflammation. Based on the biochemical parameters and renal biopsies in this study, cell infiltration and renal injury such as tubule degeneration and moderate fibrosis truly existed in the injured kidney after administration of AA for 56 days. In a previous study, inflammation markers, such as F4/80 and tumor necrosis factor-α (TNF-α), were induced in the

339 damaged kidney after long-term administration of AA [21]. On the other hand,
340 methylglyoxal is produced after injury or inflammation and is also a pro-
341 inflammatory factor. Methylglyoxal promotes inflammation via upregulating the
342 nuclear factor-kappa B (NF-κB) signaling pathway [28]. Furthermore, AGEs,
343 methylglyoxal-derivatized adducts, react with receptors for advanced glycation end
344 products (RAGE) to further evoke inflammation [32].
345 Another essential finding of this study was that the level of serum methylglyoxal
346 peaked on day 70, while the levels of MG excreted in urine were lower at this time
347 point than at day 70.These findings indirectly reflects accumulation of methylglyoxal
348 in the injured kidney. In agreement with these observations, severe renal injury and
349 interstitial fibrosis were detected at day 70. As previously described, accumulation of
350 methylglyoxal is harmful and aggravates fibrosis in a variety of pathologies [33-35].
351 The potential mechanisms include activation of transient receptor potential ankyrin 1
352 (TRPA1) [35], promotion of the cell cycle [35], differentiation of fibroblasts [33-36],
353 induction of the epithelial-mesenchymal transition (EMT) via the TGF-β/Snail axis
354 [34], and inhibition of the binding step of collagen phagocytosis [37]. Moreover,
355 Kottmann *et al.* proposed that lactic acid may activate TGF-β and lead to
356 accumulation of hypoxia-inducible factor 1-α (HIF-1α)—which promotes

357 myofibroblast differentiation—in idiopathic pulmonary fibrosis [38]. However, the
358 effects of methylglyoxal on interstitial renal fibrosis are still unknown.
359 Previous studies only assessed urinary methylglyoxal and D-lactate under injury
360 conditions, such as oxidative stress [39], inflammation [40], necrosis [14] or fibrosis
361 [20]). However, we found that urinary methylglyoxal and D-lactate remained elevated
362 at 28 days after AA withdrawal (day 84), when the severity of fibrosis and
363 tubulointerstitial injury had reduced to mild. These changes in urinary methylglyoxal
364 and D-lactate may be related to renal repair and detoxification. Generally, injured
365 tissues use glycolysis to produce energy for repair [41], thus methylglyoxal might be
366 released. Lan *et al.* detected increased levels of byproducts of glycolysis (lactate and
367 pyruvate) in the kidney during reperfusion after acute ischemia-reperfusion injury
368 [42]. Thus, methylglyoxal may be excreted into urine and metabolized into D-lactate
369 by GLO1 as a mechanism of detoxification [18]. Indeed, most studies did not assess
370 the pathological alterations after long-term withdrawal of AA. However, our
371 assessment of the changes up to 28 days after withdrawal of AA (day 84) indicate
372 repair is a time-consuming process. The association between repair and methylglyoxal
373 warrants more detailed investigation in further research. Moreover—as a limitation of
374 this study—although AA-DNA adducts are a biomarker for AA exposure and
375 urothelial cell carcinoma [43], AA-DNA adducts were not determined in this study. In

the future, AA-DNA adducts should be detected to evaluate the severity of tubulointerstitial injury.

Conclusion

Methylglyoxal is produced and exacerbates kidney injury (inflammation and fibrosis), and excretion and metabolism of methylglyoxal may represent a strategy of detoxification after injury. After withdrawal of AA, tubulointerstitial injury became mild, due to the low cumulative dose of AA. Thus, AA-containing herbs such as Xixin should be used at low doses for short durations (i.e., less than one month) and the renal function of the patients should be monitored.

List of abbreviations

AA: aristolochic acid; AAI: aristolochic acid I; AA II: aristolochic acid II; AAN: aristolochic acid nephropathy; AGEs: advanced glycation end products; BUN: blood urea nitrogen; DDP: 2,20-dipyridyl disulfide; DPDS: 6-diamino-2,4-dihydroxypyrimidine sulfate; EMT: epithelial-mesenchymal transition; FD-HPLC: high-performance liquid chromatography and fluorescence detection; GLO1: glyoxalase 1; HIF-1α: hypoxia-inducible factor 1-α; MeCN: acetonitrile; 4-MU: 4-methylumbelliferone; NAG: *N*-acetyl-β-D-glucosaminidase; NBD-PZ: 4-nitro-

7-piperazino-2,1,3-benzoxadiazole; NF-κB: nuclear factor-kappa B; OAT: organic anion transporter; PAS: periodic acid–Schiff; PTEC: proximal tubular epithelial cells; RAGE: receptors for advanced glycation end products; Scr: serum creatinine; SSAO: semicarbazide-sensitive amine oxidase; TFA: trifluoroacetic acid; THIS: tubulointerstitial histological score; TNF-α: tumor necrosis factor-α; TPP: triphenylphosphine; TRPA1: transient receptor potential ankyrin 1.

Declarations

Ethics approval and consent to participate

All animal protocols were approved by the Animal Care and Use Committee of Taipei Medical University (LAC-2019-0482).

Consent for publication

Not applicable.

Availability of data and materials

Not applicable.

Competing interests

The authors declare that they have no competing interests.

Funding

We are grateful to the financial support from the Ministry of Science and Technology, Taiwan, R.O.C. (NSC 97-2320-B-038-007-MY3).

Authors' contributions

Study design and conception of animal experiment: Shih-Ming Chen and Chia-En Lin; data collection and data analysis: Chia-En Lin, Po-Yeh Lin, Wen-Chi Yang, Tzu-Yao Lin, and Chien-Ming Chen; animal experiment: Chia-En Lin, Po-Yeh Lin, Wen-Chi Yang, Yu-Shen Huang, Tzu-Yao Lin; data interpretation: Jen-Ai Lee and Chia-En Lin; manuscript drafting: Chia-En Lin; semi-quantitative analysis for collagen deposition: Hung-Shing Chen; critical revising the manuscript: Shih-Ming Chen and Jen-Ai Lee. All authors reviewed and approved the manuscript.

Acknowledgements

We appreciate it very much that Prof Shiro Ueda provided recommendation to our animal experiments and metabolic cages for urine collection. The graphical abstract was created with BioRender.com. We are grateful to the financial support from the Ministry of Science and Technology (NSC 97-2320-B-038-007-MY3). We acknowledge UNIVERSAL LINK CO., LTD. who provided professional writing services or materials.

Footnotes

Table 1. Biochemical parameters of the normal (N) and aristolochic acid (AA) group

BUN: blood urea nitrogen; Scr: serum creatinine; NAG: *N*-acetyl-β-D-glucosaminidase; * $p < 0.05$ *vs*. N group at the same time point, Student's t-test; # $p < 0.05$ *vs.* AA group on day 56; † $p < 0.05$ *vs.* AA group on day 70, repeated measures ANOVA

Fig. 1 Periodic acid-Schiff (PAS) stained kidney sections and tubular interstitial histological scores (TIHS)

(a-i) Representative images of PAS-stained kidney sections from the N group on day 28 (a), 56 (c), 70 (e), and 84 (g) and AA group on days 28 (b), 56 (d), 70 (f), and 84 (h). The arrow indicates interstitial renal fibrosis. The stars indicate cellular infiltration. (i) Tubular interstitial histological scores (THIS). N group, normal group; AA group, aristolochic acid group. ** $p < 0.01$ *vs.* N group at the same time point, Student's *t*-test; # $p < 0.05$ *vs.* AA group on day 56. † $p < 0.05$ *vs.* AA group on day 70, repeated measures ANOVA.

Fig. 2 Masson's trichrome stained kidney sections and semi-quantitative analysis of collagen deposition

The fraction of interstitial fibrosis was assessed as the percentage of aniline blue-stained area. (a-i) Representative images of Masson's trichrome-stained kidney sections from the N group on day 28 (a), 56 (c), day 70 (e), and day 84 (g) and AA group on day 28 (b), 56 (d), day 70 (f), and day 84 (h). The arrow indicates collagen

451 deposition. (i) Semiquantitative analysis of collagen deposition. N group, normal
452 group; AA group, aristolochic acid group. ** $p < 0.01$ *vs.* N group at the same time
453 point, Student's *t*-test; # $p < 0.05$ *vs.* AA group on day 56. † $p < 0.05$ *vs.* AA group on
454 day 70, repeated measures ANOVA.
455 Fig. 3 Picro Sirius Red stained kidney sections and semi-quantitative analysis of
456 collagen deposition
457 The fraction of interstitial fibrosis was assessed as the percentage of red-stained area.
458 (a-f) Representative images of Picro Sirius Red-stained kidney sections from the N
459 group on day 28 (a), 56 (c), day 70 (e), and day 84 (g) and AA group on day 28(b), 56
460 (d), day 70 (f), and day 84 (h). The arrow indicates collagen deposition. (i)
461 Semiquantitative analysis of collagen deposition. N group, normal group; AA group,
462 aristolochic acid group. * $p < 0.05$, ** $p < 0.01$ *vs.* N group at the same time point,
463 Student's *t*-test; # $p < 0.05$ *vs.* AA group on day 56. † $p < 0.05$ *vs.* AA group on day
464 70, repeated measures ANOVA.
465 Fig. 4 Chromatograms of analysis and contents of methylglyoxal in serum and urine
466 HPLC chromatograms for serum methylglyoxal level on day 56 (a), day 70 (b), and
467 day 84 (c). The corresponding peaks of methylglyoxal derivative was labeled in
468 HPLC chromatograms. (d) Serum methylglyoxal content. The white bars indicate the
469 N group and the black bars indicate the AA group. N group, normal group; AA group,

aristolochic acid group. HPLC chromatograms for urinary methylglyoxal on day 56 (e), day 70 (f), and day 84 (g). The corresponding peaks of methylglyoxal derivative was labeled in HPLC chromatograms. (h) Urinary methylglyoxal content, calculated as methylglyoxal level × 12-h urinary volume. N group, normal group; AA group, aristolochic acid group. * $p < 0.05$ and ** $p < 0.01$ *vs.* N group at the same time point, Student's *t*-test; # $p < 0.05$ *vs.* AA group on day 56. † $p < 0.05$ *vs.* AA group on day 70, repeated measures ANOVA.

Fig. 5 Chromatographs of analysis and contents of lactate (D,L-lactate and D-lactate) in urine

(a, c, e) HPLC chromatographs for the D,L-lactate on day 56 (a), day 70 (c), and day 84 (e). (b, d, f) HPLC chromatographs for the D-lactate on day 56 (a), day 70 (b), and day 84 (c). The corresponding peaks of D,L-lactate and D-lactate derivative and internal standard (I.S.) was labeled in HPLC chromatograms. (g, h) Quantification of D,L-lactate (g) and D-lactate (h) amount. Urinary D,L-lactate amount, calculated as D,L-lactate level × 12-h urinary volume; urinary D-lactate amount, calculated as D-lactate level × 12-h urinary volume. N group, normal group; AA group, aristolochic acid group; I.S., internal standard. *** $p < 0.001$ *vs.* N group at the same time point, Student's *t*-test; # $p < 0.05$ *vs.* the AA group on day 56, repeated measures ANOVA.

Fig. 6 Western blot analysis and relative levels of glyoxalase 1(GLO1) in the kidney

489 homogenates

490 (a) Representative western blot of GLO-1; β-actin was used as an internal control. (b)

491 Semi-quantitative analysis of GLO1 expression. AA56, AA group on day 56; AA70,

492 AA group on day 70; AA84, AA group on day 84; N group, normal group; AA group,

493 aristolochic acid group. * $p < 0.05$ *vs.* N group, ANOVA.

494

495 References

496 1. Zhang C, Wang X, Shang M, Yu J, Xu Y, Li Z, et al. Simultaneous determination of

497 five aristolochic acids and two aristololactams in Aristolochia plants by high-

498 performance liquid chromatography. Biomed Chromatogr. 2006;20(4):309-18.

499 2. Vanherweghem JL, Depierreux M, Tielemans C, Abramowicz D, Dratwa M, Jadoul

500 M, et al. Rapidly progressive interstitial renal fibrosis in young women: association

501 with slimming regimen including Chinese herbs. Lancet. 1993;341(8842):387-91.

502 3. Kamei T, Kondoh T, Nagura S, Toriumi Y, Kumano H, Tomioka H. Improvement of

503 C-reactive protein levels and body temperature of an elderly patient infected with

504 Pseudomonas aeruginosa on treatment with Mao-bushi-saishin-to. J Altern

505 Complement Med. 2000;6(3):235-9.

506 4. Takagi Y, Higashi N, Kawai S, Maeda A, Ueba N. Effects of traditional oriental

507 medicine on influenza virus infection:: Activating effect of Mao–Bushi–Saishin-To

(MBST, Ma-Huang-Fu-Zi-Xin-Tang) on IgG antibody producibility in aged mice. International Congress Series. 2004;1263:670-3.

5. Oh J, Hwang IH, Kim DC, Kang SC, Jang TS, Lee SH, et al. Anti-listerial compounds from Asari Radix. Arch Pharm Res. 2010;33(9):1339-45.

6. Hashimoto K, Yanagisawa T, Okui Y, Ikeya Y, Maruno M, Fujita T. Studies on anti-allergic components in the roots of Asiasarum sieboldi. Planta Med. 1994;60(2):124-7

7. Yu HH, Seo SJ, Hur JM, Lee HS, Lee YE, You YO. Asarum sieboldii extracts attenuate growth, acid production, adhesion, and water-insoluble glucan synthesis of Streptococcus mutans. J Med Food. 2006;9(4):505-9.

8. Kim SJ, Gao Zhang C, Taek Lim J. Mechanism of anti-nociceptive effects of Asarum sieboldii Miq. radix: potential role of bradykinin, histamine and opioid receptor-mediated pathways. J Ethnopharmacol. 2003;88(1):5-9.

9. Ren M, Tang Q, Chen F, Xing X, Huang Y, Tan X. Mahuang Fuzi Xixin Decoction Attenuates Th1 and Th2 Responses in the Treatment of Ovalbumin-Induced Allergic Inflammation in a Rat Model of Allergic Rhinitis. Journal of Immunology Research. 2017;2017:8254324.

10.Zhang W, Zhang J, Zhang M, Nie L. Protective effect of Asarum extract in rats with adjuvant arthritis. Exp Ther Med. 2014;8(5):1638-42.

11.Beisswenger PJ, Drummond KS, Nelson RG, Howell SK, Szwergold BS, Mauer M. Susceptibility to diabetic nephropathy is related to dicarbonyl and oxidative stress. Diabetes. 2005;54(11):3274-81.

12.Li YC, Shih YM, Lee JA. Gentamicin caused renal injury deeply related to methylglyoxal and N(varepsilon)-(carboxyethyl)lysine (CEL). Toxicol Lett. 2013;219(1):85-92.

13.Huang YS, Li YC, Tsai PY, Lin CE, Chen CM, Chen SM, et al. Accumulation of methylglyoxal and d-lactate in Pb-induced nephrotoxicity in rats. Biomed Chromatogr. 2017;31(5).

14.Huang TC, Chen SM, Li YC, Lee JA. Urinary d-lactate levels reflect renal function in aristolochic acid-induced nephropathy in mice. Biomed Chromatogr. 2013;27(9): 1100-6.

15.Huang TC, Chen SM, Li YC, Lee JA. Increased renal semicarbazide-sensitive amine oxidase activity and methylglyoxal levels in aristolochic acid-induced nephrotoxicity. Life Sci. 2014;114(1):4-11.

16.Li YC, Tsai SH, Chen SM, Chang YM, Huang TC, Huang YP, et al. Aristolochic acid-induced accumulation of methylglyoxal and Nepsilon-(carboxymethyl)lysine: an important and novel pathway in the pathogenic mechanism for aristolochic acid nephropathy. Biochem Biophys Res Commun. 2012;423(4):832-7.

546 17.Thornalley PJ. Protein and nucleotide damage by glyoxal and methylglyoxal in
547 physiological systems--role in ageing and disease. Drug Metabol Drug Interact.
548 2008;23(1-2):125-50.
549 18.Thornalley PJ. Glyoxalase I--structure, function and a critical role in the enzymatic
550 defence against glycation. Biochem Soc Trans. 2003;31(Pt 6):1343-8.
551 19.Vander Jagt DL. Glyoxalase II: molecular characteristics, kinetics and mechanism.
552 Biochem Soc Trans. 1993;21(2):522-7.
553 20.Chen SM, Lin CE, Chen HH, Cheng YF, Cheng HW, Imai K. Effect of
554 prednisolone on glyoxalase 1 in an inbred mouse model of aristolochic acid
555 nephropathy using a proteomics method with fluorogenic derivatization-liquid
556 chromatography-tandem mass spectrometry. PLoS One. 2020;15(1):e0227838.
557 21.Lin CE, Chang WS, Lee JA, Chang TY, Huang YS, Hirasaki Y, et al. Proteomics
558 analysis of altered proteins in kidney of mice with aristolochic acid nephropathy
559 using the fluorogenic derivatization-liquid chromatography-tandem mass
560 spectrometry method. Biomed Chromatogr. 2018;32(3).
561 22.Marsilio R, Dall'Amico R, Giordano G, Murer L, Montini G, Ros M, et al. Rapid
562 determination of creatinine in serum and urine by ion-pair high-performance liquid
563 chromatography. Int J Clin Lab Res. 1999;29(3):103-9.
564 23.Sato N, Takahashi D, Chen SM, Tsuchiya R, Mukoyama T, Yamagata S, et al.

565 Acute nephrotoxicity of aristolochic acids in mice. J Pharm Pharmacol.
566 2004;56(2):221-9.
567 24.Espinosa-Mansilla A, Duran-Meras I, Canada FC, Marquez MP. High-performance
568 liquid chromatographic determination of glyoxal and methylglyoxal in urine by
569 prederivatization to lumazinic rings using in serial fast scan fluorimetric and diode
570 array detectors. Anal Biochem. 2007;371(1):82-91.
571 25.Lee J-A, Tsai Y-C, Chen H-Y, Wang C-C, Chen S-M, Fukushima T, et al.
572 Fluorimetric determination of d-lactate in urine of normal and diabetic rats by
573 column-switching high-performance liquid chromatography. Analytica Chimica
574 Acta. 2005;534(2):185-91.
575 26.Vanhaelen M, Vanhaelen-Fastre R, But P, Vanherweghem JL. Identification of
576 aristolochic acid in Chinese herbs. Lancet. 1994;343(8890):174.
577 27.Jong TT, Lee MR, Hsiao SS, Hsai JL, Wu TS, Chiang ST, et al. Analysis of
578 aristolochic acid in nine sources of Xixin, a traditional Chinese medicine, by liquid
579 chromatography/atmospheric pressure chemical ionization/tandem mass
580 spectrometry. J Pharm Biomed Anal. 2003;33(4):831-7.
581 28.Hsu Y-H, Lo C-F, Liu F-S, Lin J-H. Analysis of Aristolochic Acid in Asarum
582 (Xixin) and Its Preparations by Liquid Chromatography/Tandem Mass
583 Spectrometry. Journal of Food and Drug Analysis. 2009;17:274-81.

584 29.Cosyns JP, Dehoux JP, Guiot Y, Goebbels RM, Robert A, Bernard AM, et al.
585 Chronic aristolochic acid toxicity in rabbits: a model of Chinese herbs
586 nephropathy? Kidney Int. 2001;59(6):2164-73.
587 30.Debelle FD, Nortier JL, De Prez EG, Garbar CH, Vienne AR, Salmon IJ, et al.
588 Aristolochic acids induce chronic renal failure with interstitial fibrosis in salt-
589 depleted rats. J Am Soc Nephrol. 2002;13(2):431-6.
590 31.Lebeau C, Debelle FD, Arlt VM, Pozdzik A, De Prez EG, Phillips DH, et al. Early
591 proximal tubule injury in experimental aristolochic acid nephropathy: functional
592 and histological studies. Nephrology Dialysis Transplantation. 2005;20(11):2321-
593 32.
594 32.Rabbani N, Thornalley PJ. Glyoxalase Centennial conference: introduction, history
595 of research on the glyoxalase system and future prospects. Biochem Soc Trans.
596 2014;42(2):413-8.
597 33.Retamal IN, Hernandez R, Melo F, Zapata P, Martinez C, Martinez J, et al.
598 Glycated Collagen Stimulates Differentiation of Gingival Myofibroblasts. J
599 Periodontol. 2017;88(9):926-35.
600 34.Hirahara I, Ishibashi Y, Kaname S, Kusano E, Fujita T. Methylglyoxal induces
601 peritoneal thickening by mesenchymal-like mesothelial cells in rats. Nephrol Dial
602 Transplant. 2009;24(2):437-47.

603 35.Oguri G, Nakajima T, Yamamoto Y, Takano N, Tanaka T, Kikuchi H, et al. Effects
604 of methylglyoxal on human cardiac fibroblast: roles of transient receptor potential
605 ankyrin 1 (TRPA1) channels. Am J Physiol Heart Circ Physiol.
606 2014;307(9):H1339-52.
607 36.Yuen A, Laschinger C, Talior I, Lee W, Chan M, Birek J, et al. Methylglyoxal-
608 modified collagen promotes myofibroblast differentiation. Matrix Biol.
609 2010;29(6):537-48.
610 37.Chong SA, Lee W, Arora PD, Laschinger C, Young EW, Simmons CA, et al.
611 Methylglyoxal inhibits the binding step of collagen phagocytosis. J Biol Chem.
612 2007;282(11):8510-20.
613 38.Kottmann RM, Kulkarni AA, Smolnycki KA, Lyda E, Dahanayake T, Salibi R, et
614 al. Lactic acid is elevated in idiopathic pulmonary fibrosis and induces
615 myofibroblast differentiation via pH-dependent activation of transforming growth
616 factor-beta. Am J Respir Crit Care Med. 2012;186(8):740-51.
617 39.Chen SM, Chen TH, Chang HT, Lin TY, Lin CY, Tsai PY, et al. Methylglyoxal and
618 D-lactate in cisplatin-induced acute kidney injury: Investigation of the potential
619 mechanism via fluorogenic derivatization liquid chromatography-tandem mass
620 spectrometry (FD-LC-MS/MS) proteomic analysis. PLoS One.
621 2020;15(7):e0235849.

622 40.Lin P-Y, Chen S-M, Hsieh C-L, Lin C-Y, Huang Y-S, Hamase K, et al.
623 Determination of temporal changes in serum and urinary lactate and 3-
624 hydroxybutyrate enantiomers in mice with nephrotoxic serum nephritis by multi-
625 dimensional HPLC. Journal of pharmaceutical and biomedical analysis.
626 2020;188:113367.
627 41.Im MJ, Hoopes JE. Energy metabolism in healing skin wounds. J Surg Res.
628 1970;10(10):459-64.
629 42.Lan R, Geng H, Singha PK, Saikumar P, Bottinger EP, Weinberg JM, et al.
630 Mitochondrial Pathology and Glycolytic Shift during Proximal Tubule Atrophy
631 after Ischemic AKI. J Am Soc Nephrol. 2016;27(11):3356-67.
632 43.Stiborová M, Arlt VM, Schmeiser HH. DNA Adducts Formed by Aristolochic Acid
633 Are Unique Biomarkers of Exposure and Explain the Initiation Phase of Upper
634 Urothelial Cancer. International journal of molecular sciences. 2017;18(10):2144.

Figures

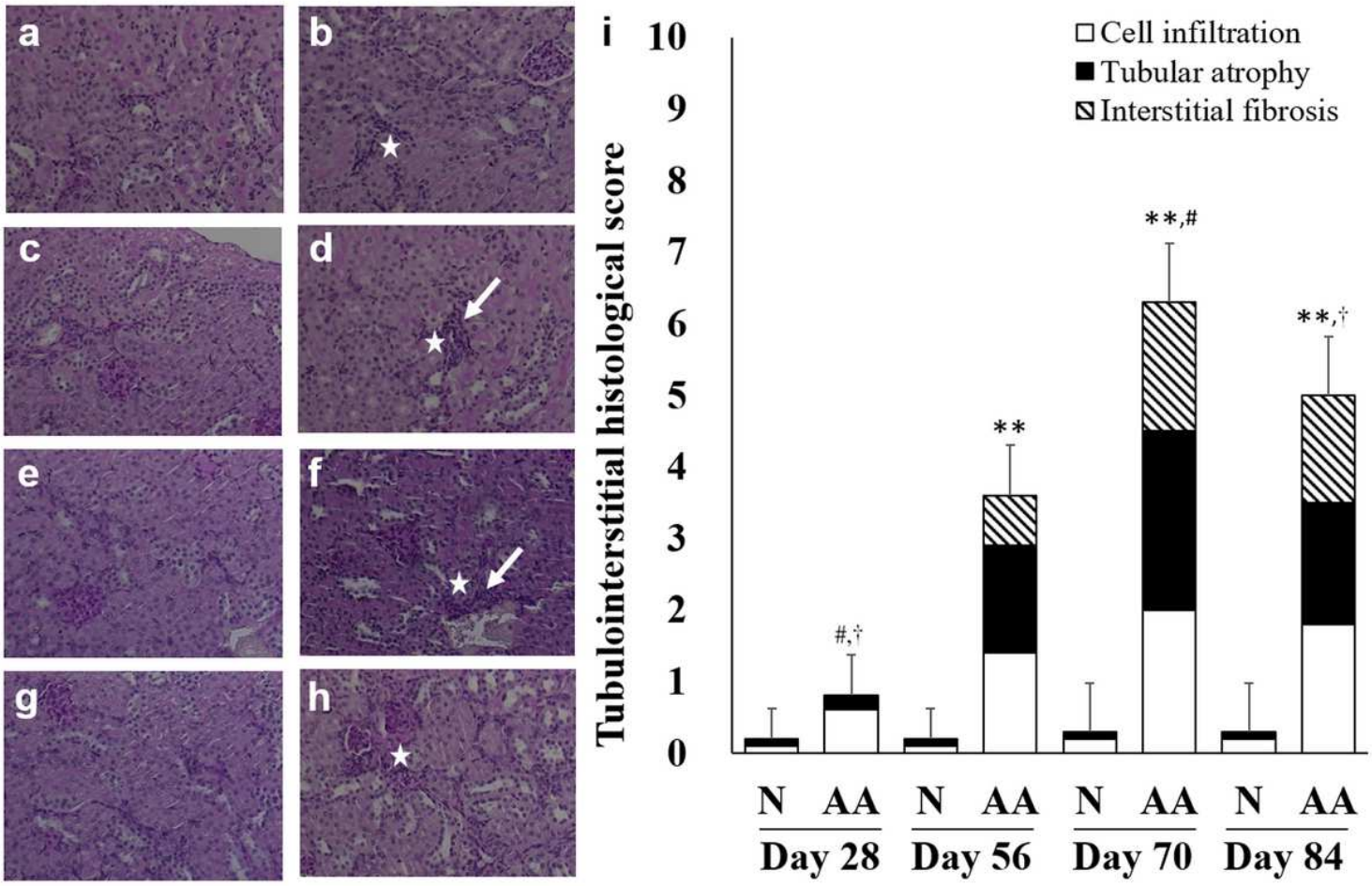

Figure 1

Periodic acid Schiff (PAS) stained kidney sections and tubular interstitial histological scores (TIHS) (a-i) Representative images of PAS stained kidney section s from the N group on day 28 (a), 56 (c), 70 (e), and 84 (g) and AA group on days 28 (b), 56 (d), 70 (f), and 84 (h). The arrow indicates interstitial renal fibrosis. The stars in dicate cellular infiltration. (i) T ubular interstitial histological scores (THIS). N group , normal group; AA group, aristolochic acid group. ** $p < 0.01$ vs. N group at the same time point, Student's t test; # $p < 0.05$ vs. AA group on day 56. $p < 0.05$ vs. AA group on day 70, repeated measures ANOVA.

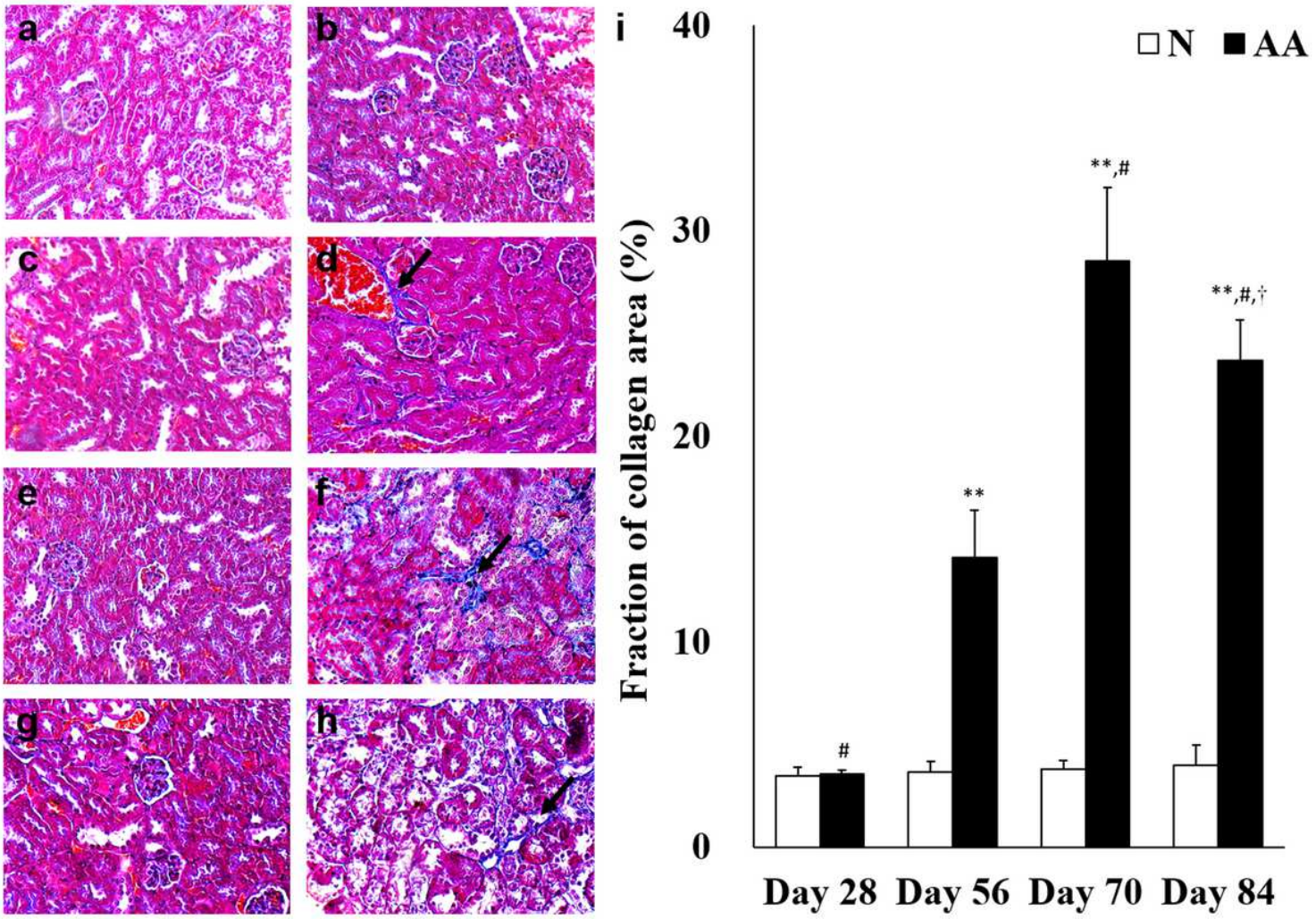

Figure 2

Masson's trichrome stained kidney sections and semi quantitative analysis of collagen deposition The fraction of interstitial fibrosis was assessed as the percentage of aniline blue stained area. (a-i) Representative images of Masson's trichrome stained kidney sections from the N group on day 28 (a) 56 (c), day 70 (e), and day 84 (g) and AA group on day 28 (b) 56 (d), day 70 (f), and day 84 (h). The arrow indicates collagen deposition. (i) Semiquantitative analysis of collagen deposition. N group , normal group; AA group, aristolochic acid group. ** $p < 0.01$ vs. N group at the same time point, Student's t test; # $p < 0.05$ vs. AA group on day 56 $p < 0.05$ vs. AA group on day 70, repeated measures ANOVA.

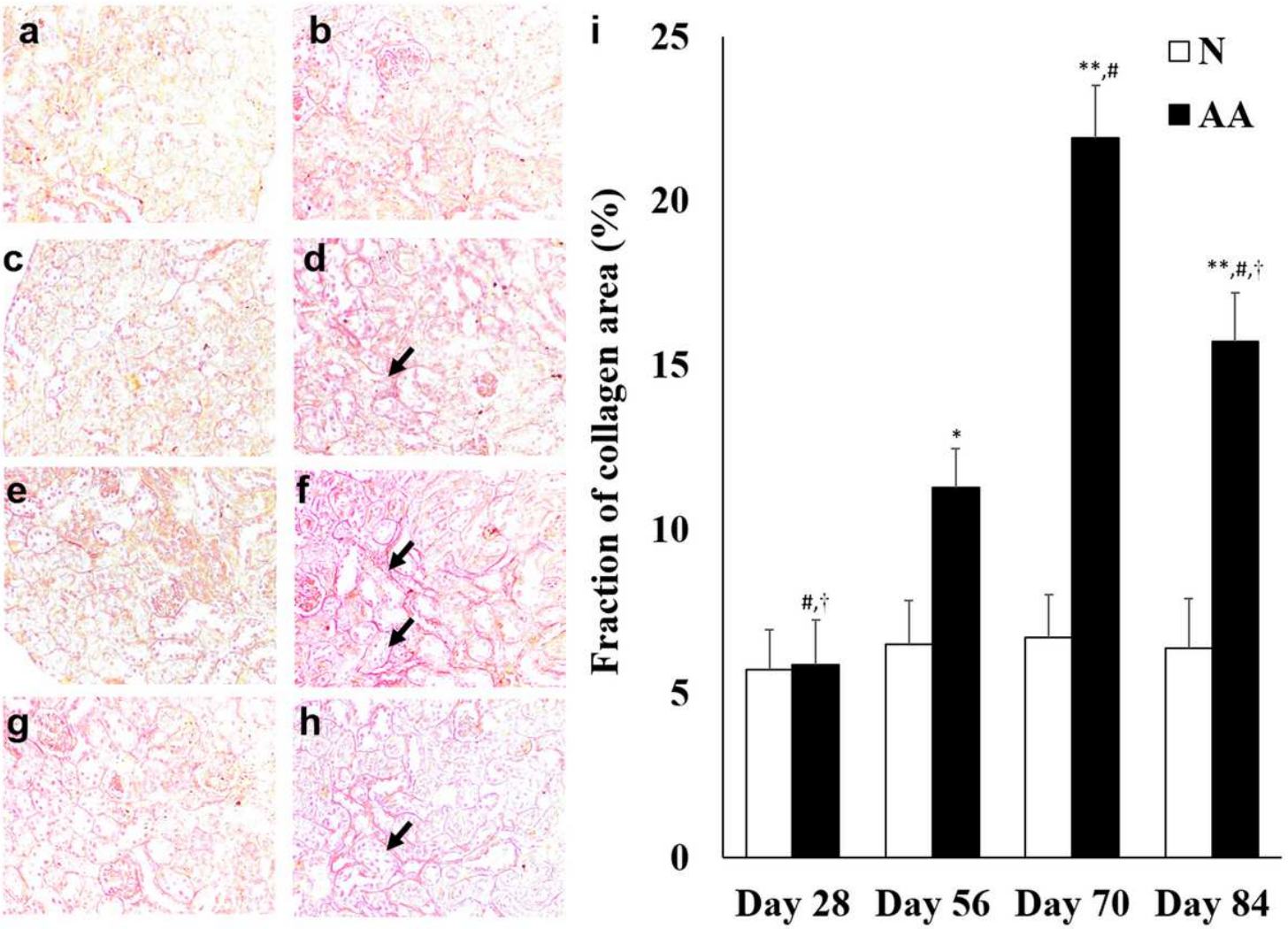

Figure 3

Picro Sirius Red stained kidney sections and semi quantitative analysis of collagen deposition The fraction of interstitial fibrosis was assessed as the percentage of red stained area. (a-f) Representative images of Picro Sirius Red stained kidney sectio ns from the N group on day 28 (a), 56 (c), day 70 (e), and day 84 (g) and AA group on day 28(b), 56 (d), day 70 (f), and day 84 (h). The arrow indicates collagen deposition. (i) Semiquantitative analysis of collagen deposition. N group , normal group; AA group, aristolochic acid group. * $p < 0.0\ 5$, ** $p < 0.01$ vs. N group at the same time point, Student's t test; # $p < 0.05$ vs. AA group on day 56. $p < 0.05$ vs. AA group on day 70, repeated measures ANOVA.

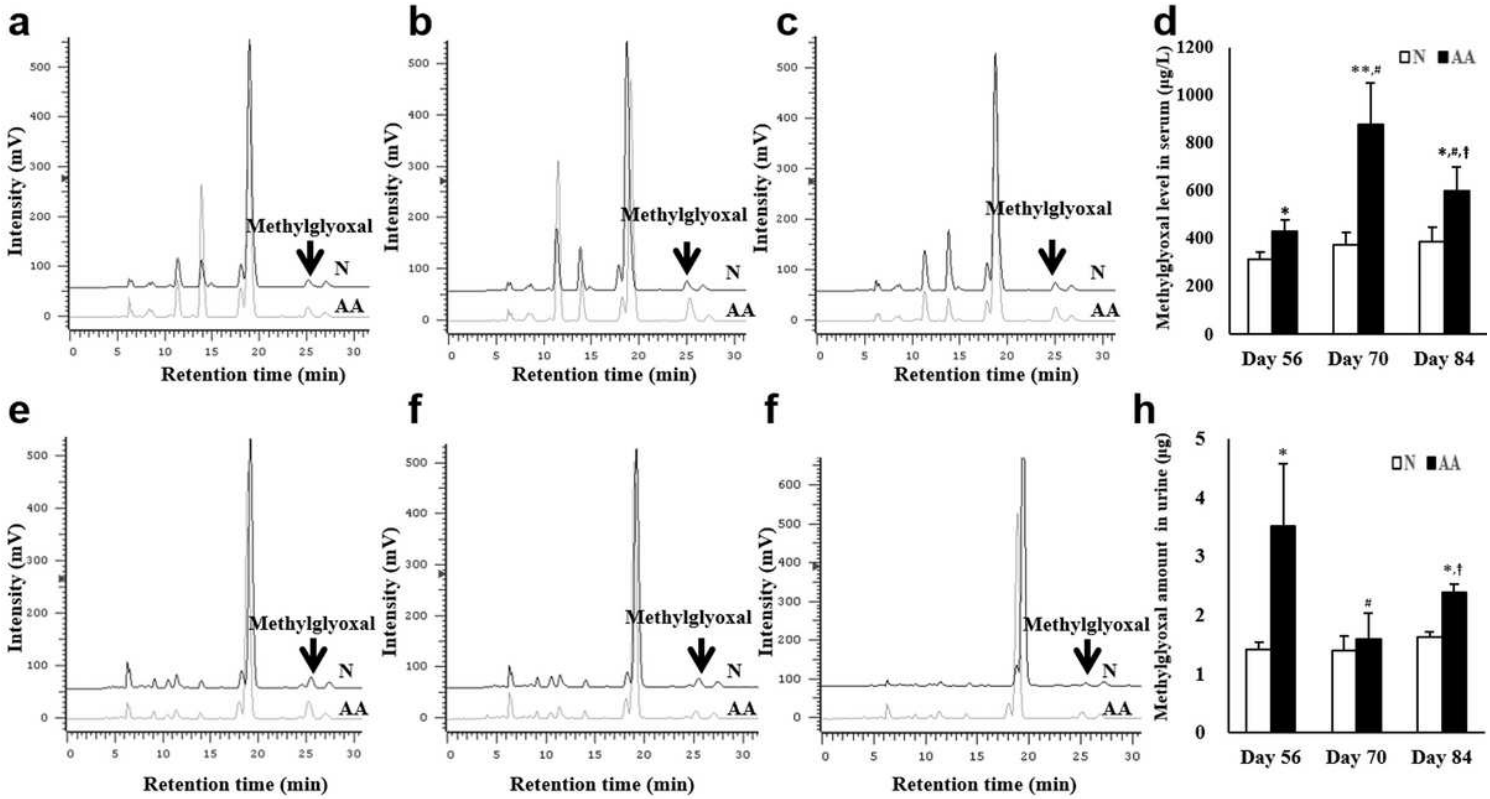

Figure 4

Chromatograms of analysis and contents of methylglyoxal in serum and urine HPLC chromatograms for serum methylglyoxal level on day 56 (a), day 70 (b), and day 84 (c). The corresponding peaks of methylglyoxal derivative was l abeled in HPLC chromatograms. (d) Serum methylglyoxal content. The white bars indicate the N group and the black bars indicate the AA group. N group , normal group; AA group, aristolochic acid group. HPLC chromatograms for urinary methylglyoxal on day 56 (e), day 70 (f), and day 84 (g). The corresponding peaks of methylglyoxal derivative was l abeled in HPLC chromatograms. (h) Urinary methy lglyoxal content , calculated as methylglyoxal level × 12 h urinary volume. N group , normal group; AA group, aristolochic acid group. * $p < 0.05$ and ** $p < 0.01$ vs. N group at the same time point, Student's t test; # $p < 0.05$ vs. AA group on day 56 † p 0.05 vs. AA group on day 70, repeated measures ANOVA.

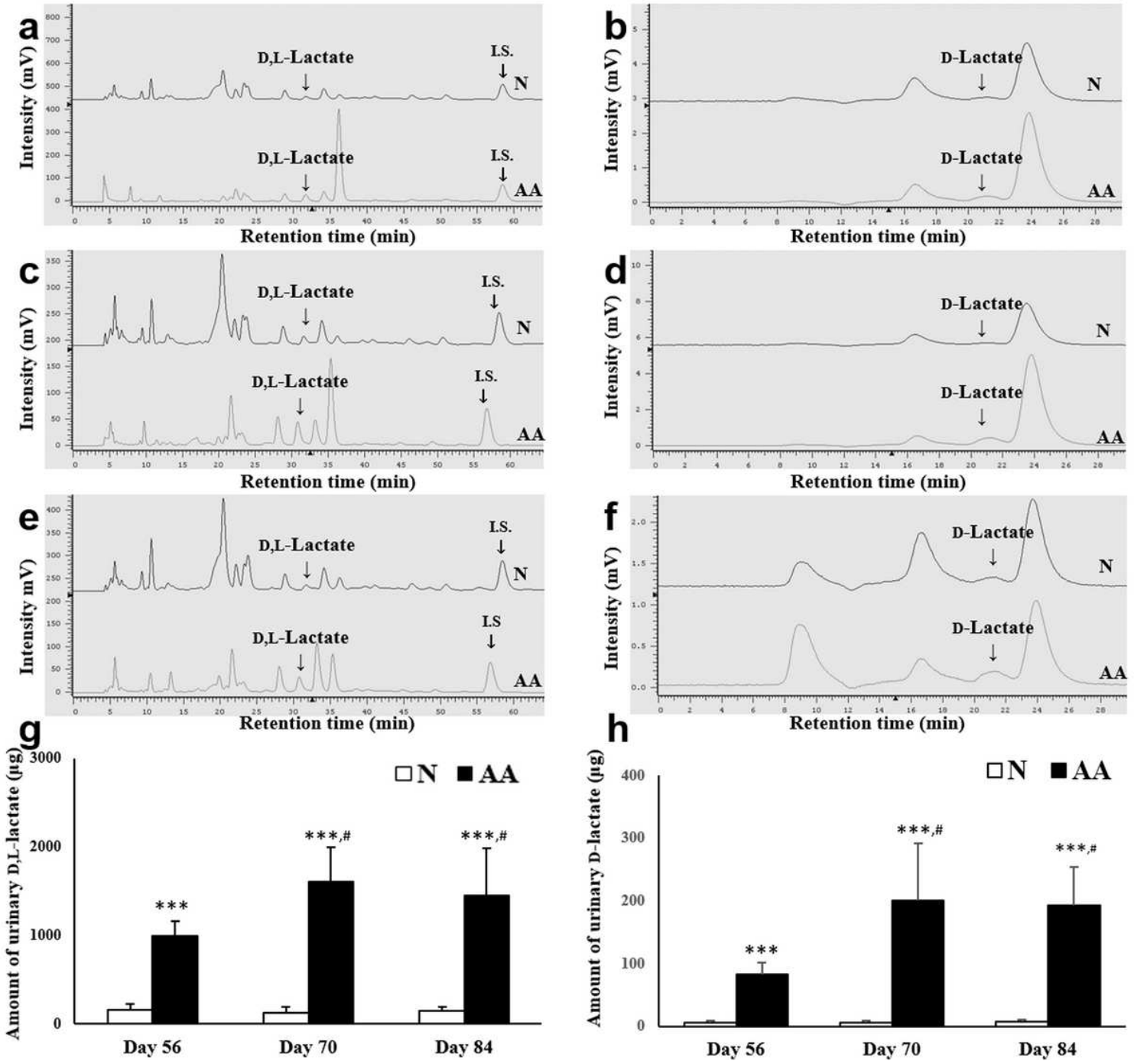

Figure 5

Chromatographs of analysis and contents of lactate (D,L lactate and D lactate) in urine (a, c, e) HPLC chromatographs for the D,L lactate on day 56 (a), day 70 (c), and day 84 (e). (b, d, f) HPL C chromatographs for the D lactate on day 56 (a), day 70 (b), and day 84 (c). The corresponding peaks of D,L lactate and D lactate derivative and internal standard (I.S.) was labeled in HPLC chromatograms. (g, h) Quantification of D,L lactate (g) and D-lactate (h) amount. Urinary D,L lactate amount, calculated as D,L lactate level × 12 h urinary volume; urinary D lactate amount, calculated as D lactate level × 12 h urinary volume. N group , normal group; AA group, aristolochic acid group; I.S., internal stan dard. *** p <

0.001 vs. N group at the same time point, Student's t test; # p < 0.05 vs. the AA group on day 56, repeated measures ANOVA.

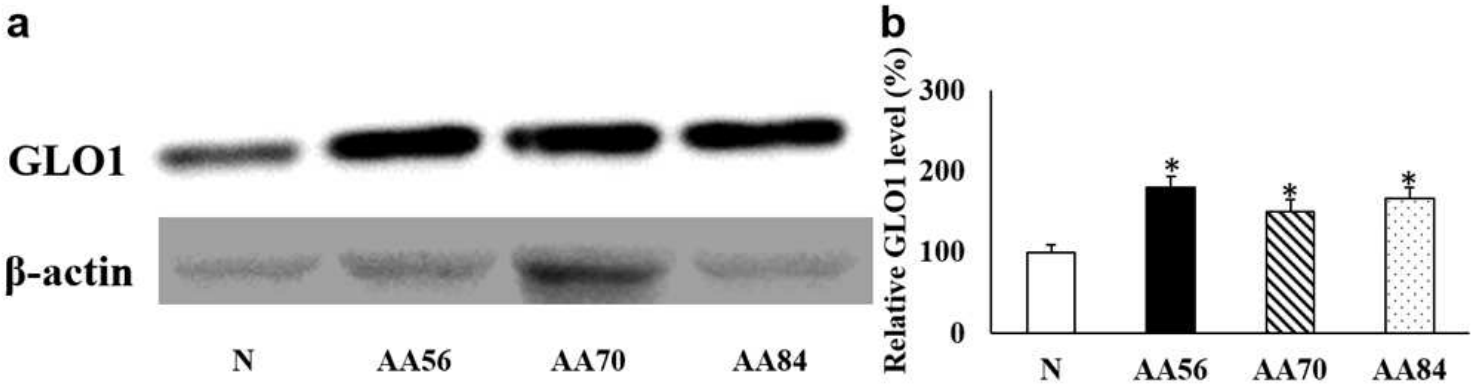

Figure 6

Western blot analysis and relative levels of glyoxalase 1(GLO1) in the kidney homogenates (a) Representative western blot of GLO 1; β actin was used as an internal control. (b) Semi quantitative analysis of GLO1 expression. AA56, AA group on day 56; AA70, AA group on day 70; AA84, AA group on day 84; N group , normal group; AA group, aristolochic acid group * p 0.05 vs. N group, ANOVA.